

Simplified tests to study the size effect of the compression chord in beams under shear forces. Application of DIC methodology

Ensayos en probetas para el estudio del efecto tamaño en la cabeza de compresión de vigas sometidas a esfuerzo cortante. Aplicación de la metodología DIC

Eva Oller^{*, a}, Cristina Barris^b, Antonio Marí^c, Lluís Torres^d y Andrés Santander^e

^a Associate Prof. Dr. Dept. of Civil and Environmental Engineering. Universitat Politècnica de Catalunya (UPC BarcelonaTech)

^b Associate Prof. Dr. Department of Mechanical Engineering and Industrial Construction. Universitat de Girona (UdG), Spain

^c Prof. Dr. Department of Civil and Environmental Engineering. Universitat Politècnica de Catalunya (UPC BarcelonaTech), Spain

^d Prof. Dr. Department of Mechanical Engineering and Industrial Construction. Universitat de Girona (UdG), Spain

^e MSc in Structural and Construction Engineering. Universitat Politècnica de Catalunya (UPC BarcelonaTech)

RESUMEN

Con el objetivo de evaluar cómo afecta el efecto del tamaño en las tensiones de la cabeza de compresión en vigas sometidas a esfuerzos cortantes, se ha desarrollado un programa experimental de 50 probetas prismáticas sometidas a un ensayo de tracción indirecta. Se han estudiado los siguientes parámetros: dimensiones, esbeltez, resistencia a compresión del hormigón y tamaño máximo del árido. Para capturar el comportamiento post-pico del hormigón, la carga se introdujo en función del ancho de fisura, a través de algoritmos de control apropiados. Se ha utilizado la técnica de correlación digital de imágenes (DIC) en 2D para capturar la formación, abertura y propagación de fisuras.

ABSTRACT

To evaluate how the size effect affects the stresses developed along the compression chord in a beams subjected to shear forces, a simplified experimental program was developed on 50 prismatic specimens subjected to a splitting test. The studied parameters were: dimensions, slenderness, concrete compressive strength, and maximum aggregate size. To capture the post-peak behavior of the concrete, the load was introduced as a function of the crack width, through appropriate control algorithms. Digital Image Correlation (DIC) in a 2D configuration has also been used to accurately capture the formation, width and propagation of cracks to corroborate the experimental measurements.

PALABRAS CLAVE: efecto tamaño, cortante, ensayo tracción indirecta, abertura de fisura, DIC.

KEYWORDS: size effect, shear, indirect tensile strength, maximum crack width, DIC

1. Introduction

The shear strength of reinforced concrete (RC) elements depends on the size of the specimen. As experimentally observed, the mean value of the shear stresses along the section

decreases with the section depth, and this is more significant in elements without transverse reinforcement [1].

The explanations for this phenomenon are usually based in one of the following two lines: a) on the one hand, the "Weibull effect" associated with the greater probability of finding defects or low resistance as the size of the element increases, an effect that would be preponderant in the lower range of dimensions [1], [2]; b) on the other hand, there are explanations based on fracture mechanics, associated with the quasi-fragile nature of the concrete and the location of the damage in an area with a finite length.

In beams under shear forces, it has been observed that failure occurs when the critical shear crack develops inside the concrete compression chord. According to Zararis and Papadakis [3], the compression chord, between the load application point and the end of the critical shear crack, behaves under a force system which is similar to that introduced in a splitting test.

2. Experimental program

The main objective of this experimental program [4] is to reproduce the behaviour of the compression chord of a beam without transverse reinforcement subjected to a shear force, when the second branch of the critical shear crack

opens and propagates just before failure (Figure 1 a). Figure 1 b shows the acting forces in the compression chord, which are similar to a Brazilian tensile test. Figure 1 c and d shows the area under study, which can be assimilated to a semi-trapezoidal element, and can be extrapolated to a prismatic specimen, simply supported in its basis, and with a linear load acting on its upper face (Figure 1 e).

Therefore, the size effect in beams subjected to shear forces is studied through indirect tensile tests in prismatic specimens with three different mean strengths (25, 40 and 60 N/mm²), different maximum aggregate sizes (12 or 20 mm) and different sizes: 100x100x100, 100x100x400, 150x150x150, 150x150x300, 150x150x600 mm [4].

In order to simulate the first critical branch, a vertical notch of 2 mm width and 30 or 45 mm depth was performed in specimens with 100 mm x 100 mm and 150 mm x 150 mm base, respectively. Nevertheless, the vertical crack did not always started at the end of the notch, especially for the tallest specimens.

Table 1 shows the main characteristics of the 50 tested specimens (concrete compressive strength f_c , maximum aggregate size a_{max} , #of tests, dimensions ($b \times b$ being $a = b$), slenderness l , supports spacing and notch length.

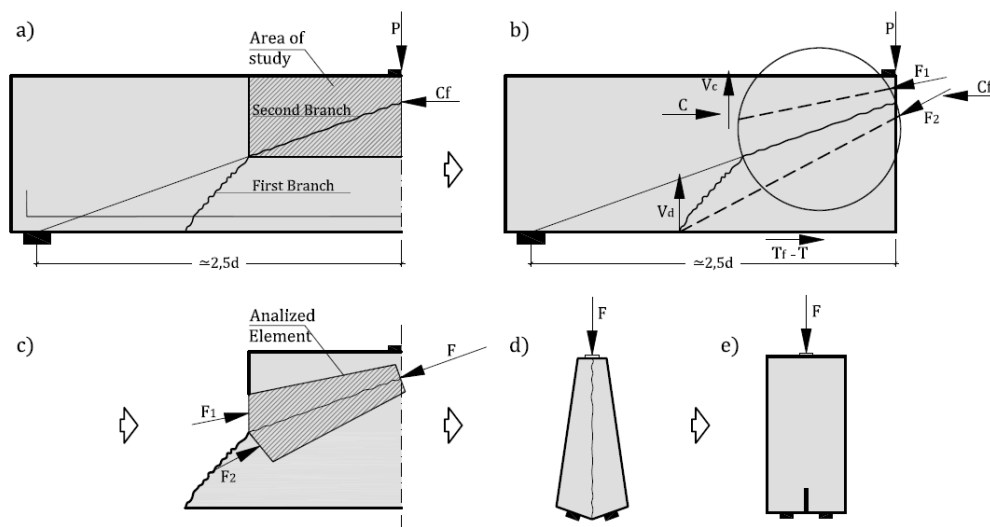


Figure 1. Modified indirect tensile test.

Table 1. Characteristics of the tested specimens.

| | f_c (N/mm ²) | a_{max} (mm) | # of tests | $b \times b$ (mm) | $\lambda = h/b$ | Supports spacing (mm) | Notch length (mm) |
|---|----------------------------|----------------|------------|-------------------|-----------------|-----------------------|-------------------|
| 1 | 25 | 20 | 10 | 100x100 | 1 | 55 | 30 |
| 2 | 40 | 12 | 10 | 150x150 | 1 | 75 | 45 |
| 3 | 40 | 20 | 10 | 150x300 | 2 | 75 | 45 |
| 4 | 60 | 12 | 10 | 100x400 | 4 | 55 | 30 |
| 5 | 60 | 20 | 10 | 150x600 | 4 | 75 | 45 |

2.1 Test set-up and instrumentation

Tests were performed with a dynamic axial test machine INSTRON 8805 with 4-column frame and ± 1000 kN actuator.

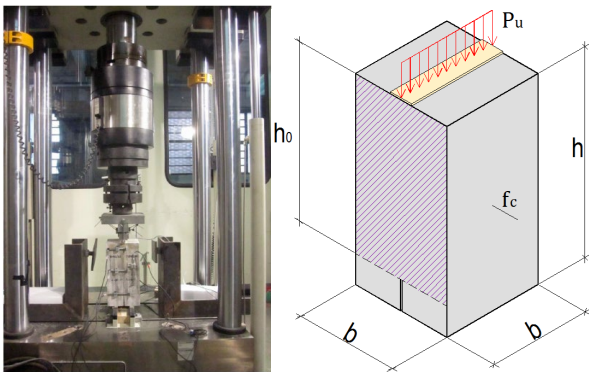


Figure 2. Test set-up.

Supports were materialized through two cylindrical bars with a spacing that depends on the specimen height.

Load was applied in a band of 30 mm width and along the dimension parallel to the notch (see Figure 2).

The instrumentation consisted in several transducer displacements (LVDT's) and a strain transducer that in the specimens of less than 300 mm height was placed at the end of the vertical notch to measure the crack width at this point. For specimens with more than 300 mm height, the strain transducer was placed at 20 mm from the top of the specimen, since the crack did not initiate at the end of the notch. Figure 3 shows the location of the instrumentation for some of the tested specimens.

Additionally to previously described instrumentation, the front surface dashed in Fig.

1 was treated so as to measure the field of displacements through digital image correlation (DIC). DIC system is a contactless measuring technique that allows obtaining displacements and deformations of a given surface. The procedure to calculate displacements is based on comparing two consecutive digital images of a given field of view (FOV) captured along the test.

In this case, a 2D configuration was used to determine the in-field displacements and therefore to measure the crack width evolution along its height with time. The DIC setup comprised two digital cameras SONY IT CCD ICS655 with a resolution of 2452x2056 pixels and an image sensor format of 8,5x7,1mm. The cameras recorded pictures at a ratio of 2 pictures/s during each test. The concrete surface where the FOV was previously defined was painted so as to obtain a random pattern of black speckles over the white surface. In order to check the contrast and density of speckles, a mean intensity gradient (MIG) [5] was calculated for all specimens, obtaining a mean value of 14,7 with a standard deviation of 3,3.

A normalized square differences correlation criterion was used to calculate the displacement of different points so as to obtain the evolution of crack width with time and along the FOV. A conversion factor varying from 0.050 to 0,1489 mm/px was obtained, and a subset size of 39 px with a step size of 9 px was used.

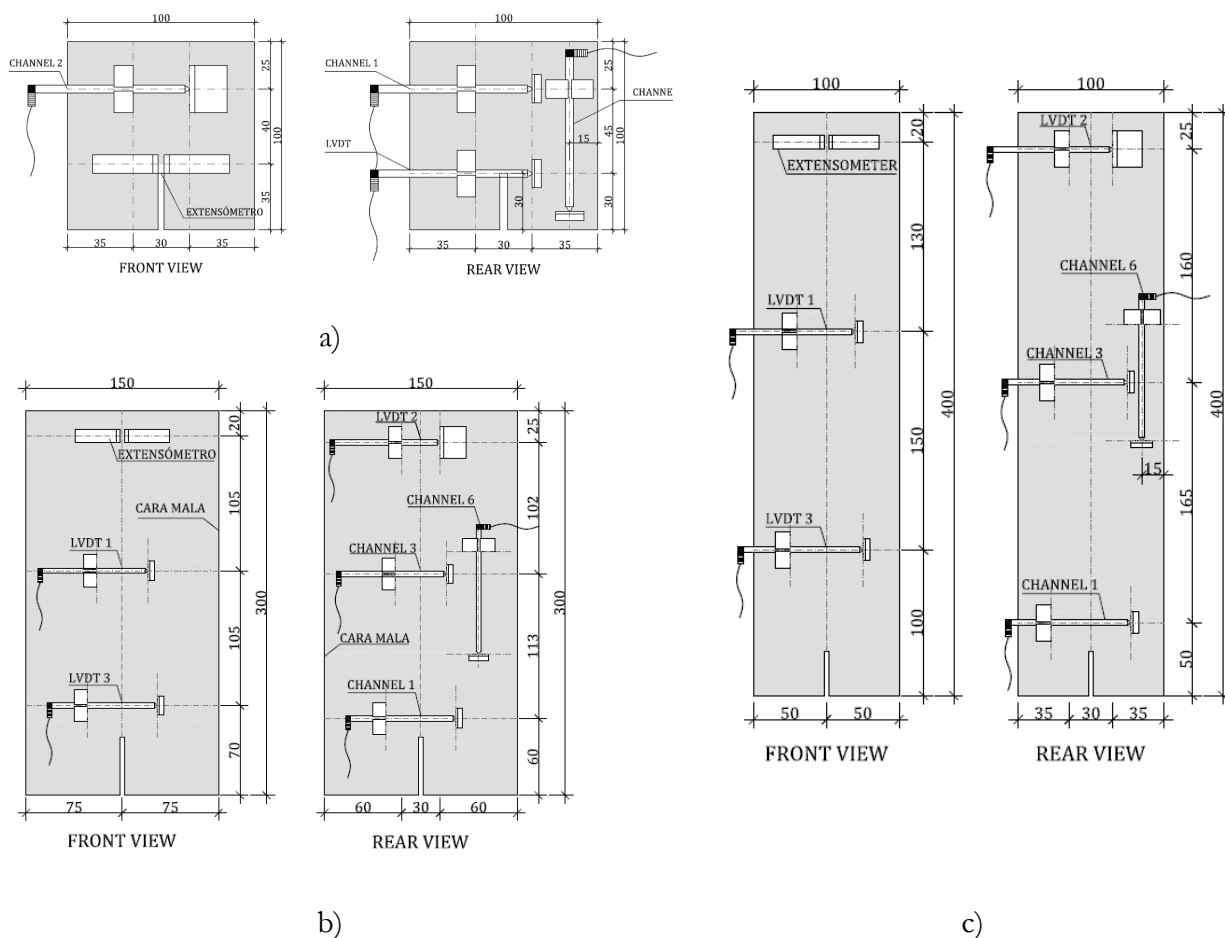


Figure 3. Instrumentation of specimens: a) 100x100x100; b) 150x150x300 mm, c) 100x100x400 mm.

3. Experimental results

3.1 Maximum load

Table 2 shows the maximum load for the 50 indirect tensile tests performed, as a function of the specimen dimensions, the concrete strength and maximum aggregate size. For each specimen two different series were tested. As observed, the maximum load increases with the height of the specimen, the concrete strength and aggregate size. As observed, the maximum loads of the specimens with 300 mm height are higher than that of specimens with 400 mm height, and in some cases very close to those of 600 m height.

Table 2. Maximum load, P_{max} (kN)

| # | Size | H25 (lateral side) | H40 (lateral side) | H40 (lateral side) | H60 (lateral side) | H60 (lateral side) |
|---|---------|--------------------------|--------------------------|--------------------------|--------------------------|--------------------------|
| | | P_{max} | P_{max} | P_{max} | P_{max} | P_{max} |
| 1 | 100x100 | 29,9 | 39,0 | 33,2 | 31,7 | 38,3 |
| 2 | | 35,0 | 31,0 | 33,1 | 39,0 | 33,0 |
| 1 | 150x150 | 53,1 | 82,1 | 74,3 | 51,7 | 75,2 |
| 2 | | 93,6 | 84,1 | 98,4 | 57,1 | 107,8 |
| 1 | 150x300 | 145,5 | 134,7 | 136,5 | 156,1 | 176,1 |
| 2 | | 139,3 | 147,1 | 148,2 | 148,7 | 158,9 |
| 1 | 100x400 | - | 64,6 | 94,2 | 89,8 | 89,1 |
| 2 | | 85,2 | 67,1 | 80,8 | 86,8 | 97,5 |
| 1 | 150x600 | 131,6 | 144,0 | 160,5 | 162,1 | 154,9 |
| 2 | | 150,3 | 136,6 | 169,8 | 159,4 | 183,5 |

3.2 Size effect

In order to represent the size effect, a non-dimensional load is defined as shown in Equation (1) to compare the results of all tests.

$$\sigma = \frac{P_{max}}{f_c b h_0} \quad (1)$$

where: P_{max} is the maximum load, f_c is the mean value of the compression strength the day of the test, b is the specimen width and h_0 is the distance between the end of the notch and the top fibre of the specimen.

As observed in Figure 4, there is a size effect trend, since the non-dimensional load asymptotically decreases with the height of the specimen. In addition, there are some unexpected values for the specimen of 150x150x150 mm. The specimens of 150x150x300 mm show a non-dimensional load higher than the trend given by other specimens.

Specimens with the same concrete strength show similar results in spite of the maximum aggregate size. This indicates that this parameter has not a direct influence in the size effect.

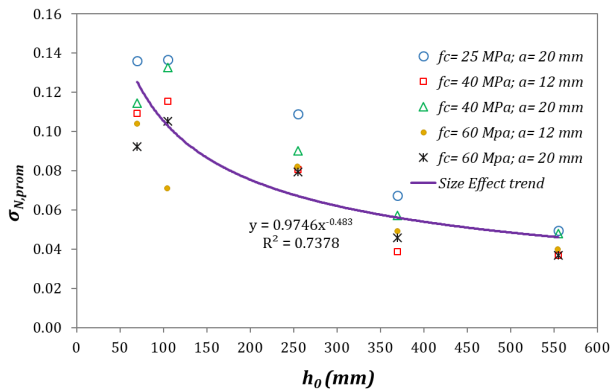


Figure 4. Size effect.

The mean value of the non-dimensional strength can be represented as shown in Eq. 2. As observed, the trend depends on the inverse of almost the square root effective height h_0 , as predicted by fracture mechanics, Bazant [2].

$$\sigma_{N,mean} = 0,975h_0^{-0.483} \quad (2)$$

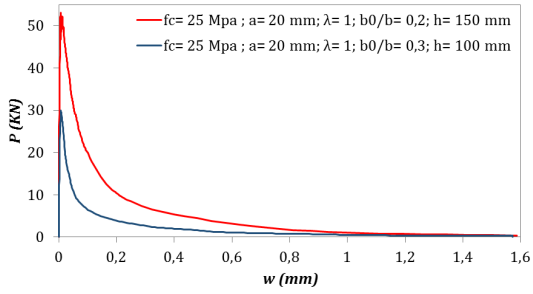
3.3 Influence of different parameters

This section studies the influence of some parameters such as specimen height b (100, 150, 300, 400 and 600 mm), maximum aggregate size a_{max} (12 and 20 mm), concrete strength f_c (25, 40 y 60 N/mm²) and slenderness λ (1, 2 and 4) through the relationship between the applied load and the crack width. As observed in Figure 5, the initial branch for all specimens is almost vertical up to the maximum load corresponds to the linear elastic behaviour of the concrete. In Figures 5a, 5c, 5e, 5g and 5i, where the height of specimen is lower than 150 mm, the trend of the descending branch is similar reaching an almost zero value of the applied force for the maximum crack width.

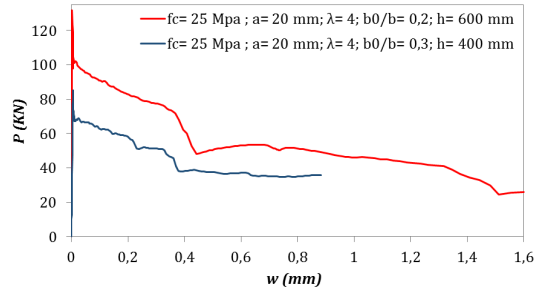
As observed in Figures 5b, 5d, 5f, 5h and 5j, the descending branch is non-uniform and it does not reach a zero value for the applied load when increasing the crack width up to its maximum value.

When analysing the influence of the maximum aggregate size, there are only slight differences, so this parameter has not a significant influence in the size effect.

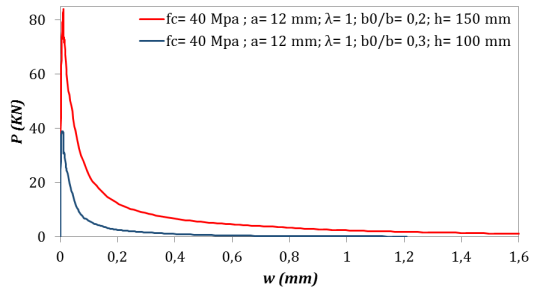
In general, for the shortest specimens (100, 150 mm or 300 mm height), the behaviour of the elements with the same height but different compression strength is quite similar. However, for specimens with 400 or 600 mm depth, the applied load and the response is higher for the 60 MPa specimen than for lower values of strength. Therefore, the higher the concrete strength, the higher the fracture energy stored under the curve.



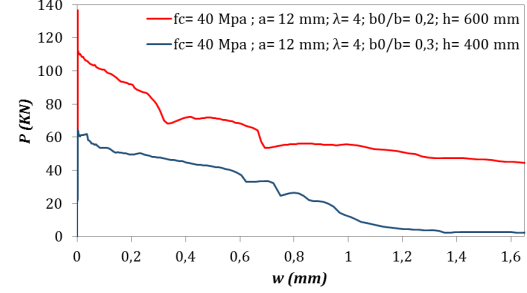
a)



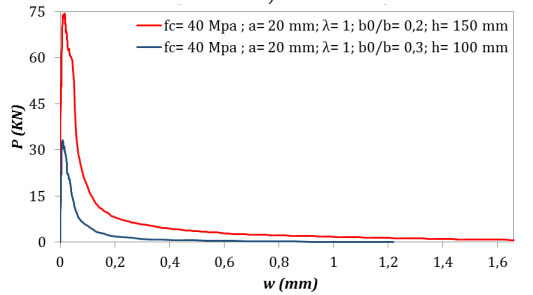
b)



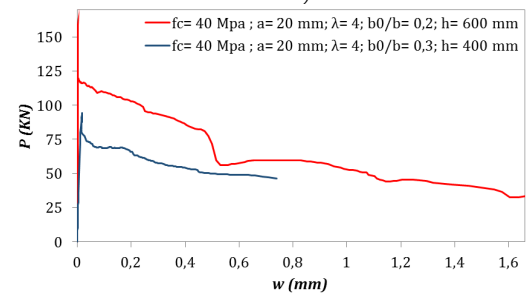
c)



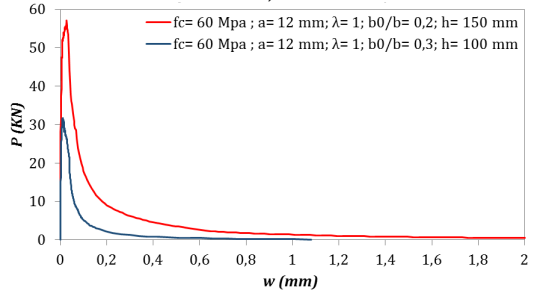
d)



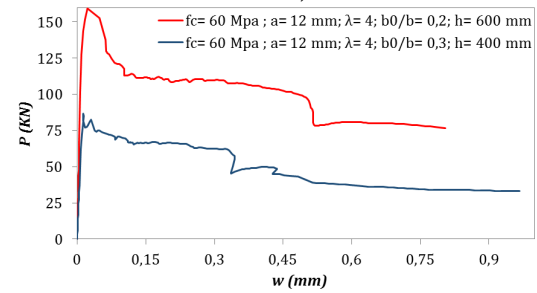
e)



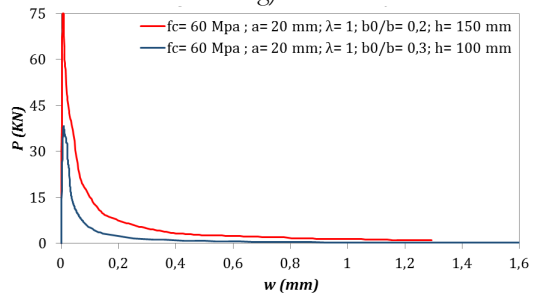
f)



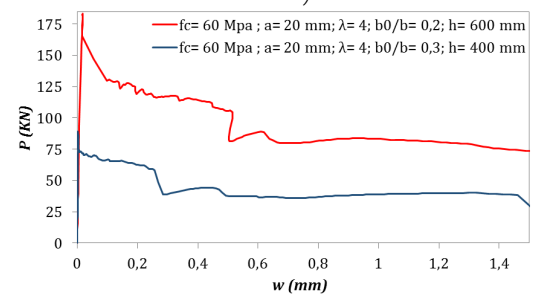
g)



h)



i)



j)

Figure 5. Load vs crack width

For 25 N/mm², Figure 6 shows the influence of the slenderness in the load vs crack width for specimens with $b=100$ mm (Fig. 6a) and $b=150$ mm (Fig. 6b). As observed, the descending branch is more uniform for a slenderness value of 1 than for specimens with a value of 4. For the highest value of slenderness ($\lambda=4$), the maximum applied load is 2.5 times the load of the same specimen with $\lambda=1$. The difference is less remarkable for specimens with $\lambda=2$. A similar trend is observed for specimens

with 60 N/mm². The main difference is the maximum load which is higher for this case.

As a conclusions, the difference between specimens with slenderness (λ) values, equal to 1 and 4 is remarkable and obvious. However, this difference is lower between elements with slenderness values of 2 and 4, in which the maximum loads are quite similar.

As observed, most of the specimens showed a maximum crack width higher than 1,50 mm, in particular those specimens with the highest slenderness value.

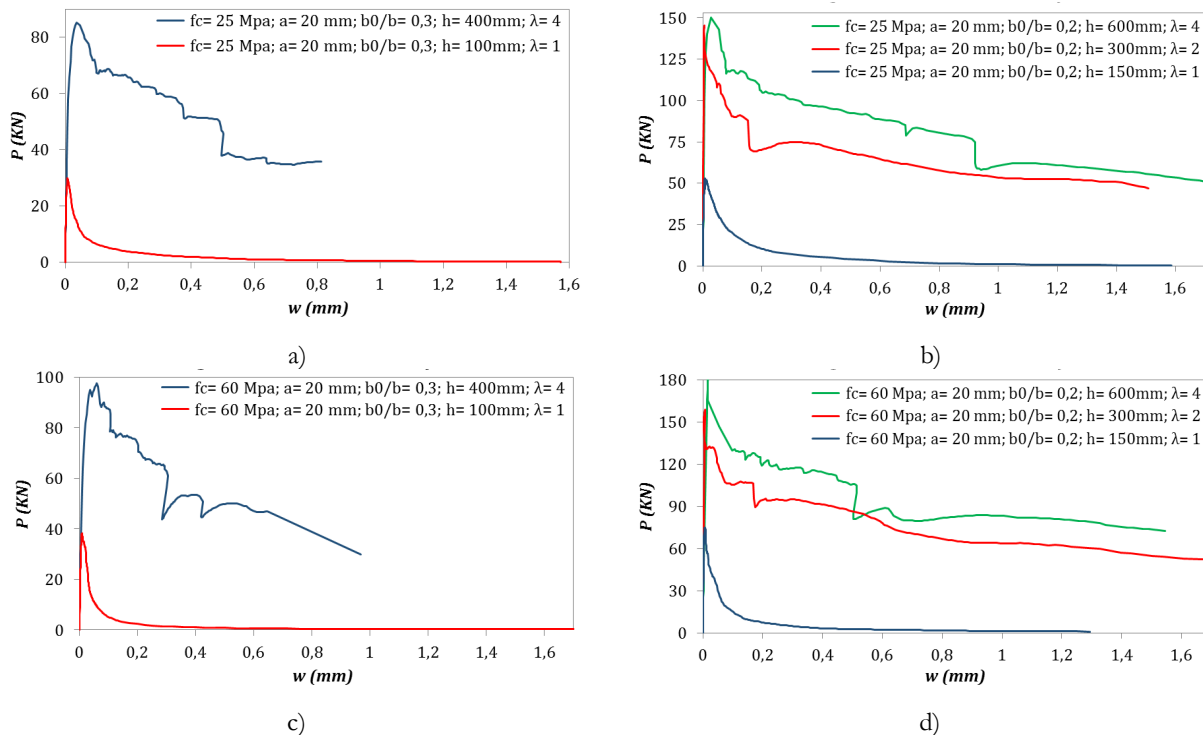


Figure 6. Load vs crack width for different slenderness values

3.4 DIC results and comparison with conventional instrumentation

In this section, the displacement results obtained with DIC are first compared with the displacements obtained by the transducers.

Then, DIC results are further explored and the evolution of crack width at different heights and with time is represented.

Crack width is calculated by DIC system as the difference between the displacements of two points, each of them located at one side of the

crack and at a fixed horizontal distance of 10 mm far from the crack width. In Figure 7, the crack width obtained with DIC at the height of the transducer is compared with that obtained by the strain transducer in specimen H40/20-150x150x150 and H40/20-100x100x400. A good fit between both results is clearly obtained.

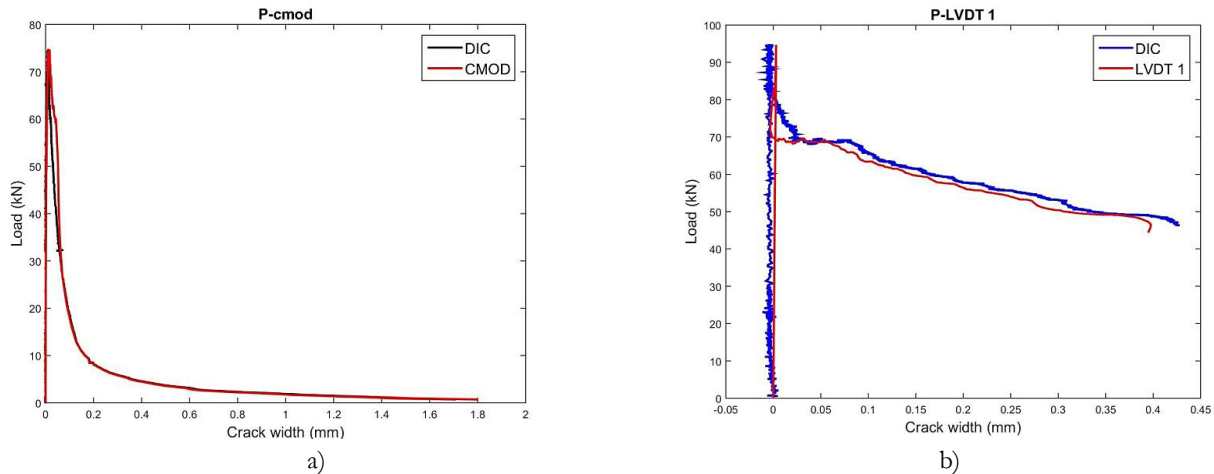


Figure 7. Load vs crack width: comparison between DIC and CMOD results, a) H40/20-150x150x150, b) H40/20-100x100x400

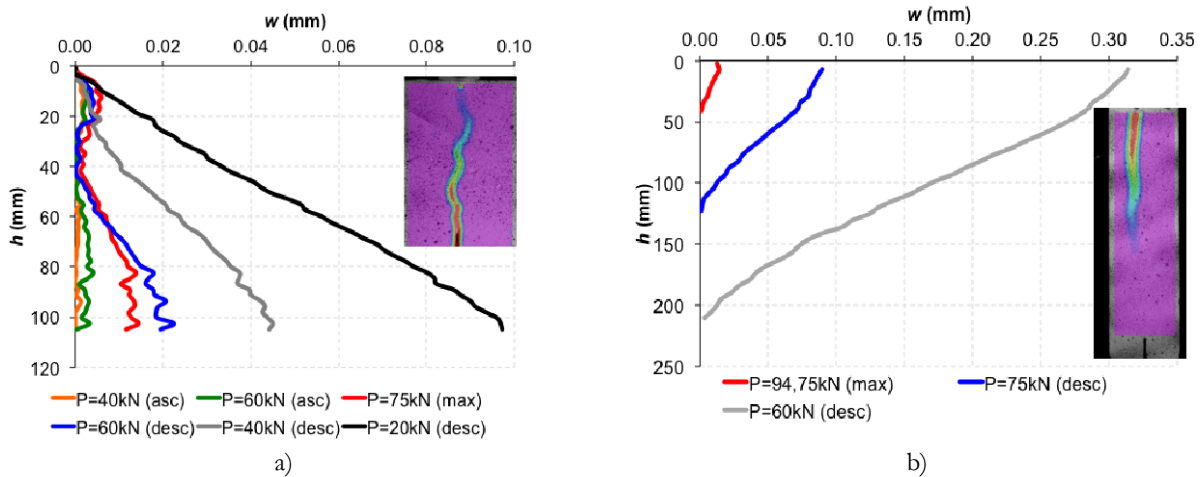


Figure 8. Crack width along the height of the specimen at representative load stages, a) H40/20-150x150x150, b) H40/20-100x100x400

In order to better investigate the evolution of crack width with height and time, the crack width calculated according to DIC results is represented along the height of the specimen at representative load stages in Figure 8 for the previously mentioned specimens.

Figure 8a shows the crack width evolution at the load where the ascending branch equals to 40kN, 60kN and 75kN (being this value the

These differences were attributed to the fact that the DIC system was measuring the crack width at one side of the specimen whilst the LVDT was placed at the opposite side.

maximum load) together with that at a load in the descending branch of 60kN, 40kN and 20kN. It is observed that, in general, crack width increases with the load, as expected, and with height. However, it is worth to mention that at first stages of loading, a slight crack opening is observed at the first 20 mm, which, with load increase, does not develop.

Figure 8b, in turn, shows the crack opening with load and height for the descending

branch of loading of specimen HA40/20-100x100x400. It is observed that, in this case, the crack starts opening from the top of the specimen and grows towards the bottom.

4. Conclusions

This paper presents an experimental program of indirect tensile tests on 50 prismatic specimens to study the size effect in the compression chord of beams without transverse reinforcement.

A size effect trend was observed since the non-dimensional maximum load decreases with the total height of the specimen.

The influence of some parameters such as specimen dimensions, concrete strength, maximum aggregate size and slenderness have been studied. From the analysis of the tests results, it can be concluded that the concrete strength has a significant influence on the maximum load only for the tallest specimens and that the aggregate size does not affect the performance of the specimens. Finally, specimens with slenderness values of 1 and 4 show a different response. However, the performance of specimens with a slenderness value of 2 is more similar to that with a slenderness value of 4.

Finally, DIC technique was applied to some of the tested specimens. As observed, the crack width obtained with the DIC system is quite similar to that obtained with the strains transducers. This fact shows the potential of the 2D DIC system to study in detail the performance of the tested specimens.

Acknowledgements

The financial support provided by the Spanish Ministry of Economy and Competitiveness (MINECO) and the European Funds for Regional Development (FEDER), through the Research projects: BIA2015-64672-C4-1-R and

BIA2017-84975-C2-2-P and through the Excellence network BIA2015-71484-REDT.

References

- [1] Z.P. Bazant, Fracture and size effect in concrete and other quasibrittle materials, Florida, 1998.
- [2] Z.P. Bazant, Size effects on structural strength: a review, Arch Appl. Mech. 69 (9-10) (199) 703–725.
- [3] P.D. Zararis and G.C. Papadakis, Diagonal shear failure and size effect in RC beams without web reinforcement, Journal of Structural Engineering. 127 (2001) 733–742.
- [4] A. Santander, Estudio experimental del efecto tamaño en probetas prismáticas de hormigón ensayadas a tracción indirecta, MSc Thesis, Universitat Politècnica de Catalunya, Barcelona, Spain, 2017.
- [5] B. Pan, Z. Lu, H. Xie, Mean intensity gradient: An effective global parameter for quality assessment of the speckle patterns used in digital image correlation. Optics and Lasers in Engineering (2009) 48, 469-477.